UCSF
UC San Francisco Previously Published Works

## Title
Microfluidic platform for rapid measurement of transepithelial water transport

## Permalink
https://escholarship.org/uc/item/0kd2p7sf

## Journal
Lab on a Chip, 17(5)

## ISSN
1473-0197

## Authors
Jin, Byung-Ju
Verkman, AS

## Publication Date
2017-02-28

## DOI
10.1039/c6lc01456a

Peer reviewed

eScholarship.org Powered by the California Digital Library
University of California

Author Manuscript

Author Manuscript

Author Manuscript

Author Manuscript

HHS Public Access

Author manuscript

*Lab Chip*. Author manuscript; available in PMC 2018 February 28.

Published in final edited form as:

*Lab Chip*. 2017 February 28; 17(5): 887–895. doi:10.1039/c6lc01456a.

# Microfluidic platform for rapid measurement of transepithelial water transport

**Byung-Ju Jin**[a] and **A.S. Verkman**[a]

[a]Departments of Medicine and Physiology, University of California, San Francisco, CA 94143-0521, U.S.A

## Abstract

Water transport across epithelial monolayers is of central importance in mammalian fluid homeostasis, and epithelial aquaporin (AQP) water channels are potential drug targets. Current methods to measure transepithelial water permeability based on indicator dilution have limited accuracy and can require hours for a single measurement. We report here a microfluidics platform for rapid and accurate measurement of water transport across a conventionally cultured epithelial monolayer on a porous filter requiring only a single image obtained using a standard laboratory fluorescence microscope. The undersurface of a porous polyester filter containing cultured epithelial cells on top is contacted with a perfused microfluidic channel of 100-μm width, 20-μm height and 10-cm length with folded geometry, with in-plane size of 3.2 × 3.2 $mm^2$ for visualization with a 2x objective lens. Osmotic water permeability is measured from the steady-state concentration profile along the length of the channel of a membrane-impermeant fluorescent dye in the perfusate, in which an osmotic gradient is imposed by an anisosmolar solution overlying the epithelial monolayer; diffusional water permeability is measured using a $D_2O/H_2O$-sensing fluorescent dye in the perfusate with a $D_2O$-containing isosmolar solution overlying the cell layer. Permeability values are deduced from single fluorescence images. The method, named Fluid Transport on a Chip (FT-on-Chip), was applied to measure transepithelial osmotic and diffusional water permeability in control and AQP4-expressing epithelial cell monolayers. FT-on-Chip allows for rapid, accurate and repeated measurements of transepithelial water permeability, and is generalizable to transport measurements of ions and solutes using suitable indicator dyes.

## Graphical Abstract

Corresponding author: Alan S. Verkman, M.D., Ph.D., 1246 Health Sciences East Tower, University of California San Francisco, CA 94143-0521, U.S.A.; Phone 415 476-8530; Fax 415 665-3847; Alan.Verkman@ucsf.edu; http/www.ucsf.edu/verkman.

Author Manuscript Author Manuscript Author Manuscript Author Manuscript

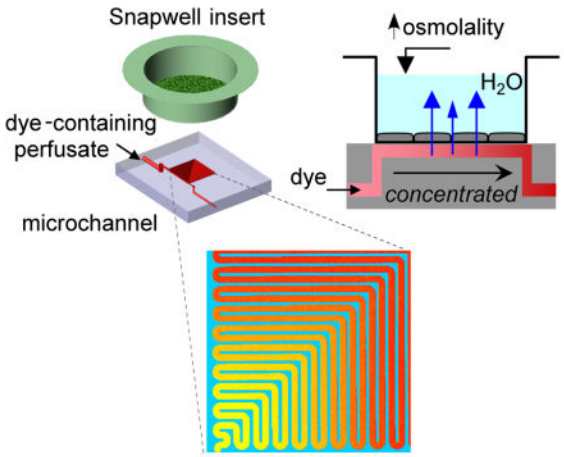


Fluid transport on a chip (FT-on-Chip) allows for rapid, accurate and repeated measurements of transepithelial water permeability

**Keywords**

water permeability; aquaporin; microfluidic channel; epithelium

## Introduction

Water transport across epithelial cell layers is of central importance in normal mammalian physiology and disease. For example, water transport by kidney tubules is required for the formation of a concentrated urine; epithelial water secretion is required for secretion of saliva and cerebrospinal fluid; and alveolar absorption of excess lung water prevents pulmonary edema. In many epithelia water transport is facilitated by aquaporin (AQP) water channels, which function as conduits to increase water flow in response to osmotic gradients created by solute transport.[1,2] Quantification of water permeability across epithelia is important in understanding fluid homeostasis in health and disease, and in evaluation of candidate drug modulators of AQP water channel function, which may have broad clinical applications.[3–5]

Water permeability measurement across epithelial cell monolayers is different from that in individual cell plasma membranes for which different measurement methods are available.[3] Osmotic water permeability across cell plasma membranes is measured from the kinetics of cell volume change in response to an osmotic gradient. Rapid changes in cell volume can be deduced by various optical methods such as light scattering, phase-contrast imaging, and volume-sensing fluorescent reporters such as calcein and chloride-sensing yellow fluorescent proteins.[6–8] Transport of water across epithelial cell layers can occur by transcellular and paracellular routes, with the transcellular route involving transport through serial apical and basolateral plasma membranes and cytoplasm. There may be extracellular unstirred layers as well. Hence, it is not possible to deduce transepithelial water permeability from measurements on cell plasma membranes, though independent measurements of

Author Manuscript Author Manuscript Author Manuscript Author Manuscript

transepithelial and cell membrane water permeabilities are useful to study transcellular vs. paracellular transport and non-membrane resistances to water flow.

The conventional approach to measure osmotic water permeability ($P_f$) across epithelial monolayers, as depicted in Fig. 1A, is to expose the epithelium to an osmotic gradient using solutions of different osmolalities bathing the opposing surfaces. Osmotically driven water transport is typically measured from the kinetics of change in the concentration of a volume marker in the solution bathing the apical surface. For flat monolayers, such as epithelial cells cultured on a porous membrane, a single measurement can require hours because of the low surface-to-volume ratio of the system. This approach has been used to measure water permeability in epithelial cell layers and to test putative AQP inhibitors,[9,10] but even with repeated fluid sampling over time the precision of deduced permeability values is poor because of volume marker binding, focal disruptions in epithelial barrier function over many hours, and other technical issues. Alternative approaches involve capacitance measurements in Ussing chambers[11] as an indicator of transepithelial volume transport, and direct volume measurement by confocal imaging;[12,13] however, each has significant limitations. In closed epithelial fluid sacs, such as toad urinary bladder and mammalian gallbladder, water permeability has been measured by serial bladder weights[14] or by fluorescence quenching of an entrapped volume indicator.[15] Flow-tube methods in the older literature,[16] which utilize narrow-bore tubes (to sense volume movement optically) connected to an Ussing chamber containing the epithelial cell monolayer, can in principle enable time-resolved measurements of osmotic water permeability, though the method is technically tedious and fraught with temperature-gradient and membrane-movement artifacts.

A second parameter describing the water permeability of a cell membrane or epithelium is the diffusional water permeability ($P_d$), which provides a measure of diffusional water exchange in the absence of net volume transport. $P_d$ has been measured from $^3H_2O$ transport across an epithelial cell layer in which radioactivity is measured in sampled fluid over time.[17] $P_f$, $P_d$ and the $P_f/P_d$ ratio provide information about the molecular nature of the water pathway and extracellular barriers to water flow such as unstirred layers.

Here, we describe a microfluidics platform for accurate water transport measurements across epithelial monolayers, which requires only a single fluorescence image. The principle of this approach was motivated by kidney tubule perfusion studies in the older literature, which involved perfusion of ~30–60 μm diameter tubules and assay of perfusate composition of collected fluid,[18,19] and by advances in our lab to image fluorescent dyes in perfused kidney tubules.[20] The idea, as depicted in Fig. 1B, is to greatly increase surface-to-volume ratio by using a long (~10-cm length) and shallow (20-μm height) microfluidic channel that is continuously perfused and subjected to an osmotic (or diffusional) gradient by using different solutions in the perfusate (bathing the epithelial basolateral surface) and bath (bathing the epithelial apical surface). Transepithelial water transport produces a predicted steady-state fluorescence profile along the axis of the channel from which water permeability is deduced. A folded channel geometry was used (Fig. 1B, bottom) in order to image a sufficient channel length to deduce water permeability at physiological water transport rates. A significant technical challenge was enabling tight contact of an epithelial cell culture on a commercial Snapwell insert (circular porous filter with plastic side walls)

Author Manuscript Author Manuscript Author Manuscript Author Manuscript

with a perfused microfluidic channel. Our approach, named Fluid Transport on a Chip (FT-on-Chip), was validated and applied to measure osmotic and diffusional water permeability in epithelial cell cultures.

## Methods

### Microfluidic channel design and fabrication

The microchannel was fabricated using conventional soft lithography with film mask printing, master fabrication and PDMS (polydimethylsiloxane) replication molding processes:[21,22] (i) microchannel design and printing on a film mask with 25,400 dpi resolution (CAD/Art Services Inc., Bandon, OR); (ii) master fabrication with 20-μm height single layer on a 4-inch silicon wafer (Addison Engineering Inc., San Jose, CA) using SU-8 2015 negative photoresist (Microchem Corp., Westborough, MA) with 2000 rpm spin-coating; and (iii) replica PDMS channel fabrication. Replica PDMS channels were molded on the silicon wafer with two PDMS layers: the first layer, which directly contacts the porous membrane of the Snapwell insert, was molded by pouring a 20:1 mixture of PDMS base and curing agent (DA-184A and DA-184B, Dow Corning, Midland, MI), followed by overnight room temperature incubation, which formed a soft and sticky PDMS layer with sub-millimeter height; the second, supporting layer was molded by pouring a 5:1 mixture of the base and curing agent on the first layer, followed by 30-min incubation at 80 °C, which gives a PDMS layer of ~0.5-cm height. The two layer PDMS replica was peeled off of the wafer. Inlet and outlet ports were created using a 0.75-mm diameter punch (Harris Uni-core - 0.75, TedPella Inc., Redding, CA) to make a ~2-mm depth vertical hole; a 1.2-mm diameter punch (Harris Uni-core - 1.2) was used to create a horizontal side hole connecting with the vertical hole. Tubing was inserted in the side inlet hole.

### Microfluidics platform setup

The microfluidics chamber was connected with a 50-μL Luer-lock glass syringe (SGE Analytical Science, Austin, TX) using Teflon tubing (1521 Tubing, IDEX Health & Science, Rohnert Park, CA) and polyethylene tubing (BTPE-50, Instech, Plymouth Meeting, PA) and connectors (P-659 and F-331Nx, IDEX Health & Science, Rohnert Park, CA). The glass syringe was driven by a syringe pump (KDS 200, KD Scientific, Holliston, MA). The microfluidic chamber was immobilized on a slide glass with the open microchannel side facing up, and mounted on the stage of an inverted epifluorescence microscope (ECLIPSE TE2000-U, Nikon, Melville, NY)

Cells were cultured on Snapwell inserts (0.4-μm pore size, tissue culture treated, 12-mm diameter, 6-well, Corning, NY) with polyester membrane. To construct the chamber the bottom of an insert was gently dried with regular lab tissue paper and placed on top of the channel. A 50-g weight was placed on top of the Snapwell insert to immobilize the device during measurement and ensure water-tight contact. Images were recorded using an EMCCD camera (Digital camera C9100, Hamamatsu, Japan). The entire channel was imaged using a 2× magnification lens (CFI60 Plan Apochromat Lambda 2x, numerical aperture 0.1, working distance 8.5 mm, Nikon).

Author Manuscript Author Manuscript Author Manuscript Author Manuscript

### Transepithelial water transport measurements

Osmotic water permeability ($P_f$) across an epithelial cell monolayer was determined as depicted in Fig. 1B. After setting up the system, the inlet was perfused at 10 μL/h with a cell-impermeant, photostable, inert dye (fluorescein dextran 500 kDa, Molecular Probes, Eugene, OR) in PBS, which filled the entire channel within ~2 min without leakage. No dye photobleaching or phototoxicity was seen as evidenced by the insensitivity of fluorescence profiles to illumination intensity and their constancy over time. The perfusate flow rate was then reduced to 0.5–10 μL/h. Following stabilization of the system for 5 min, the isosmolar PBS solution in the Snapwell compartment (~300 μL volume) was replaced by an anisomolar solution (such as PBS containing raffinose) to impose a transepithelial osmotic gradient. Fluorescence images (500 × 500 pixels) were captured at specified times at 2x magnification. Images were analyzed using Matlab (The Mathworks, version 7.1, Natick, MA) to determine the fluorescence intensity profile, *F(x),* along the axis of the channel. Fluorescence profiles were area-integrated along the length of the channel, and divided by a control profile measured prior to replacement of apical solution PBS with an anisomolar solution.

Diffusional water permeability ($P_d$), which quantifies the diffusional movement of water across an epithelial monolayer in the absence of an osmotic gradient, was measured using the $D_2O$-sensitive fluorescence dye aminonapthalene trisulfonic acid (ANTS, Molecular Probes Inc.)[23] in the isosmotic $H_2O$ PBS perfusate. An isosmolar $D_2O$ solution (same composition as PBS but with $D_2O$ replacing $H_2O$) was added in the Snapwell compartment to drive diffusional water movement, and ANTS fluorescence (excitation 385 nm, emisson 510 nm) in the channel was imaged.

### Computation of osmotic and diffusion water permeability

The transepithelial osmotic water permeability coefficient ($P_f$, in cm/s) was computed from measured *F(x)* in experiments in which the perfusate contained a volume marker as described above,

$$P_f = Q_o\,(dF/dx)_o/(v_w\,W\,\Delta Osm) \quad (1)$$

where $Q_o$ is the perfusate flow rate, $v_w$ is the partial molar volume of water (18 $cm^3$/mol), W is the channel width, and ΔOsm is the osmotic gradient across the cell monolayer. See Supplementary Information for derivation of equation (1).

Transepithelial diffusional permeability ($P_d$, in cm/s) was computed from measured *F(x)* in experiments in which the perfusate contained ANTS as described above. $D_2O$ concentration ($C_{D2O}(x)$) was computed from *F(x)* as reported:[23] $F(x) = (0.387\,C_{D2O}(x)^2 + 0.300\,C_{D2O}(x) + 0.307)/0.307$, enabling determination of $P_d$ by exponential regression,

$$C_{D2O(x)}/C_{D2O}{}^{well} = 1 - \exp\{-P_d\,(W/Q_o)\,x\} \quad (2)$$

Author Manuscript Author Manuscript Author Manuscript Author Manuscript

where $C_{D2O}^{well}$ is the (constant) $D_2O$ concentration in the Snapwell insert. See Supplementary Information for derivation of equation (2).

## Computational modeling

Computational modeling is needed for design optimization and rigorous validation of the system. Finite-element simulations were done using COMSOL Multiphysics (version 3.4; COMSOL, Burlington, MA). For fluid dynamics modeling (see Supplementary Information for full mathematical description and boundary conditions), the relatively large Snapwell compartment was modeled as a well-mixed solution with fixed concentration boundary condition. The volume flux into the insert at the interface, $J_v$, depends on the transepithelial water permeability and the osmolality difference,

$$J_v(x) = P_f \, v_w \, S \, \Delta Osm(x) \quad (4)$$

where S is the surface area of porous membrane. The spatial fluorescence profile in the microfluidic channel, *F(x,z)* (see Fig. 3), is determined by diffusion and advection as specified by an equation for solute advection-diffusion coupled with the Navier-Stokes equation describing the fluid flow field. The fluid dynamics modeling computed *F(x,z)* as a function of $P_f$, the transepithelial osmolality difference (ΔOsm), and the perfusate flow rate ($Q_o$). The computation time to obtain the steady-state solution was ~ 30 min for ~ 410,000 mesh element size, as performed on a HP Z600 workstation (Intel Xeon(R) E5645 CPU and 32G RAM, HP, Palo Alto, CA).

## Particle streak velocimetry

Fluorescent particles (1 μm, Fluoro-Max™ G0100, Thermo Scientific, Waltham, MA) were injected in the microchannel at constant flow (0.1–10 μL/h) for imaging of particle streak lines using 10× or 20× objective lenses with camera exposure times of 20–200 ms. Velocities were calculated by dividing the length of each streak-line by the exposure time. The length of particle streak lines is heterogeneous because of the parabolic velocity profile in the microchannel, with maximum velocity at the channel center. The maximum velocity was deduced using in-focus streak lines at the channel center in x-y plane. A total of 50 particle streak lines were used for each velocity calculation (see Supplementary Video 2 for particle streak images).

## Cell culture

Fisher rat thyroid (FRT) cells expressing water channel aquaporin-4 (AQP4), and control non-transfected cells, were used as described.[9,24] Cells were cultured on Snapwell inserts for 4–5 days (transepithelial resistance was > 3 kΩ·cm$^2$) in F-12 modified Ham's medium (Sigma-Aldrich, St. Louis, MO) supplemented with 10% fetal bovine serum, 2 mM glutamine, 100 units/ml penicillin, 100 μg/ml streptomycin, and 200 μg/ml G-418.

Author Manuscript Author Manuscript Author Manuscript Author Manuscript

### Transepithelial electrical resistance (TEER)

TEER was measured before and after experiments using a conventional measurement system (Millicell ERS-2, EMD Millipore, Billerica, MA) according to manufacturer's protocol. The cell culture insert with cells and a blank insert without cells were measured separately, and TEER determined from the difference. The unit area resistance is obtained by multiplying the meter reading by the surface area of the filter membrane (~1.13 $cm^2$).

## Results

### Microfluidic channel design

An important design criterion for the microfluidic channel was a large surface area for transepithelial fluid transport compared with channel volume to give an adequate change in volume marker fluorescence. As diagrammed in Fig. 1B (bottom), a long, folded channel with minimal height (20 μm) gave the required large surface-to-volume ratio. The total length of the folded channel was ~10 cm, which allow full-field (3.2 × 3.2 mm square) image capture using a 2× magnification lens. The channel width was 100 μm with 50-μm gaps between channels.

The channel layout was designed so that fluid flow filled the channel from the bottom left corner to the top right corner to enable measurements in the early-filling area with higher magnification lenses. The bridge channel connecting the inlet hole and the main channel was designed to be very narrow and short (width 25 μm, length < 1 mm) compared to the main channel (100 μm width) to minimize fluid transport outside of the central measurement area (Fig. 1B (bottom), which was confirmed experimentally from the insensitivity of fluorescence at the start of the channel to apical solution osmolality (not shown).

### Microfluidic channel characterization

Fig. 2A shows a Snapwell insert, containing a porous filter with cultured cells, mounted on the PDMS microfluidic channel. Fig. 2B shows the rectangular 3-dimensional profile of fluorescent dye in the microfluidic channel as visualized by confocal microscopy, with similar profiles obtained when the channel was contacted with a cell-containing Snapwell porous membrane or with a rigid glass slide.

It was important to maintain water-tight contact between the PDMS channel and the undersurface of the porous membrane of the Snapwell insert in which epithelial cells are pre-cultured on the top surface. We found that stable contact could be achieved using a polyester porous membrane making contact with the microfluidic channel, which was fabricated using a 20:1 ratio of Sylgard 184 base and curing agent to create a sticky PDMS layer. The injected fluorescent dye filled the entire channel within 2 min at 10 μL/h flow rate without dye leakage (Fig. 2C, left); higher flow rates up to 50 μL/h were tolerated without dye leakage or damage to the cell layer, though at 100 μL/h flow there was dye leakage and/or partial disruption of the cell layer due to the hydrostatic pressure gradient, with dye seen entering the apical chamber.

Author Manuscript Author Manuscript Author Manuscript Author Manuscript

Further characterization of the channel was done using Particle Streak Velocimetry. Particle velocities measured in the microfluidic channel in contact with the cell-containing Snapwell porous membrane were not different from those measured with the porous membrane replaced by a glass slide (Fig. 2D). As expected, velocity was linear with perfusate flow rate.

One important issue for application of FT-on-Chip for epithelial fluid transport measurement was formation and maintenance of a tight monolayer. The resistance was maintained at > 3 $k\Omega \cdot cm^2$ during device operation.

## Computational modeling of osmotic water flux

A fluid dynamics computation was done to verify absence of significant spatial solute gradients in the 20-μm channel z-direction (channel height) under the conditions of the measurement. Fig. 3A shows the computational geometry and mesh density (see Supplementary Information for mathematical description). Fig. 3B (left) shows pseudocolor images of major osmotic solute A ($C_A$) and volume marker dye B ($C_B$) in the microfluidic channel, indicating absence of concentration gradients in the channel z-direction, which is the consequence of efficient diffusional mixing (Pe < 1 along the channel height). Additional computations showed absence of solute concentration gradients for wide range of physiologically plausible parameter sets of flow rates, diffusion coefficients and water permeabilities, indicating that solutions are well mixed in the microfluidic channel in the z-direction. For a very low $D_B$ of $5\times10^{-11}$ $m^2/s$ a spatial gradient in the z-direction is predicted by the model (Fig. 3B, right), which is consequence of slow dye diffusion.

Additional computations were done for rigorous validation of the system. Fig. 3C shows computed fluorescence profiles for indicated osmotic gradients (left), perfusate flow rates (center), and osmotic water permeability coefficients (right). As expected, the spatial fluorescence profiles show the greater fluorescence changes along the 10-cm length of the channel for higher osmotic gradients, slower flow rates, and higher osmotic permeabilities.

## Osmotic water transport measurement

FT-on-Chip was used to measure transepithelial osmotic water transport. In response to a transepithelial osmotic gradient most water moves through the cell across serial apical and basolateral membranes, with a small amount of water moving between cells in the paracellular pathway.[25,26] A transepithelial osmotic gradient was imposed using an anisosmolar solution overlying the apical epithelial surface in the Snapwell insert. Solution osmolality was increased by addition of the membrane-impermeant sugar raffinose.

Fig. 4A (left) shows pseudocolor images of fluorescence in the microfluidic channel for different osmotic gradients produced by raffinose addition. While fluorescence did not change in the absence of an osmotic gradient, osmotic gradients produced increasing fluorescence along the length of the channel as water movement out of the channel resulted in dye concentration (see Supplementary Fig. S3 for details of image analysis). Fig. 4A (right) shows the deduced fluorescence, $F(x)$, along the length of the 10-cm channel. As expected, dye concentration was increased for higher osmotic gradients.

Author Manuscript Author Manuscript Author Manuscript Author Manuscript

Fig. 4B shows the dependence of *F(x)* on perfusate flow rate. At low flow rate fluorescence increased strongly along the length of the channel. As expected, the fluorescence increase is blunted at higher flow rates because of the reduced fluid residence time in the channel. The small hydrostatic pressure gradient produced by channel perfusion has negligible effect on transepithelial water transport (see Supplementary Information for quantitative analysis).

### Osmotic permeability in aquaporin-4 expressing cells

FT-on-Chip was used to measure the transepithelial osmotic water permeability ($P_f$) in FRT cells expressing AQP4 water channels, which facilitate transcellular water transport (Fig. 5A, left). Immunofluorescence in Fig. 5A (right) shows a plasma membrane pattern of AQP4 expression in the FRT-AQP4 cells.

Fig. 5B shows the pseudocolor images of microchannel fluorescence for an osmotic gradient in (non-transfected) FRT and FRT-AQP4 cells. The fluorescence profile, *F(x)*, shows greater change along the length of channel for FRT-AQP4 cells than the non-transfected FRT cells (Fig. 5C, left). Effects of the greater water permeability in FRT-AQP4 cells were also seen by visualization of streak lines in fluorescent bead studies (Supplementary Video 2). Fig. 5C (right) shows the deduced $P_f$ as determined from *F(x)*, which was ~3-fold greater in FRT-AQP4 cells than in (non-transfected) FRT cells, in agreement with prior data obtained using the conventional dye dilution method.[9] The relatively low absolute $P_f$ values for filter-grown cells is probably due to the resistance in the small space between the filter substrate and the cell layer[27] as well as the porous membrane in which pores occupy only ~0.5% of the surface.

### Diffusional permeability measurement

FT-on-Chip was also applied to measure transepithelial diffusional water permeability ($P_d$). Fig. 6A shows a schematic of the measurement method in which a $D_2O/H_2O$-sensing fluorescent dye (ANTS) is present in the perfusate and a $D_2O$-containing isosmolar solution contacts the epithelial apical surface. ANTS fluorescence along the length of channel was increased by transepithelial $H_2O/D_2O$ exchange. Fig. 6B shows the pseudocolor images of microchannel fluorescence for different concentration of $D_2O$ overlying the cell layer. As expected, the fluorescence increase was greater for the higher $D_2O$ concentration.

Fig. 6C shows deduced *F(x)* for measurements done with three $D_2O$ percentages. Of note, ANTS fluorescence is a non-linear function of $D_2O$ concentration, which accounts for curve shape and amplitude. Transepithelial $P_d$ values determined from *F(x)* were in the range 1.9–$2.0 \times 10^{-5}$ cm/s for the $D_2O$ percentages of 100, 50, 25 %. The lower $P_d$ than $P_f$ measured above is a consequence of extracellular unstirred layer effects as expected for this type of system.

## Discussion

The FT-on-Chip method reported here allows for rapid and accurate measurement of transepithelial water permeability in epithelial cell layers cultured on commercially available Snapwell filters in which permeability is deduced from a single fluorescence image obtained using a standard laboratory microscope imaging system. The microfluidics design uses a

Author Manuscript Author Manuscript Author Manuscript Author Manuscript

continuously perfused, shallow and long folded channel to increase effective surface-to-volume ratio to enable informative permeability data from a single fluorescence image. Unlike prior dye dilution or gravimetric methods that can require measurements over hours, determination of transepithelial water transport by FT-on-Chip can be done rapidly and with high accuracy, allowing resolution of the kinetics of transepithelial permeability in response to pharmacological or other maneuvers. The FT-on-Chip methodology developed here should be broadly useful because of its simplicity, speed and accuracy, and its applicability to measure transport of fluid or any substance for which a suitable fluorescent indicator exists.

The optimal channel geometry (surface-to-volume ratio) of the channel depends on water permeability, perfusate flow rate and osmotic gradient. The current design (20-μm height, 10-cm length), as characterized computationally as shown in Fig. 3, gives a robust fluorescence signal change over the 10-cm channel length for 0.5 μl/h perfusate flow rate and 300 mOsm osmotic gradient. In the current device, we estimate ~ $10^{-5}$ cm/s as the lowest detectable water permeability measured using the lowest practical flow rate of 0.1 μl/h, a 300 mOsm osmotic gradient, and a 10% fluorescence signal change at the end of the channel.

The most significant technical challenge here was enabling water-tight contact between the porous filter containing cultured epithelial cells and the PDMS microfluidic channel in order to prevent perfusate leakage, which enables the coupling of a microfluidic channel with a conventional cell culture. Tight contact between PDMS and various smooth, dry, clean and rigid surfaces, such as glass or plastic, or flexible PDMS, can be accomplished by plasma treatment; however, plasma treatment could not be used here because of damage to the cells pre-cultured on the porous filters. We initially evaluated the tightness of contact for commercially available porous membranes, including polycarbonate, polytetrafluorethylene and polyester, and found that polyester porous membranes produced consistent tight contact with a PDMS microchannel fabricated with a smooth and sticky surface. Alternative methods were also established for other types of porous membranes, including a ‘PDMS glue method’ and ‘convex microfluidic method’ as described in the Supplementary Fig. S1. In addition to their utility for different types of porous membranes, these methods may also enable contacting a microfluidic channel with live tissues for measurement of transepithelial fluid transport.

Numerous applications of FT-on-Chip are possible in addition to measurement of transepithelial osmotic and diffusional water transport. Measurement of active transepithelial fluid absorption or secretion can be done with a volume marker approach as used here for measurement of osmotic water permeability. With suitable ion- or solute-sensing fluorescent indicators in the perfusate, transport of ions and solutes is measurable, such as of protons/bicarbonate (using pH indicator), sodium, potassium, chloride, calcium and others. Parallel multiplexed measurements are possible of several transport processes using indicator dyes of different colors and multi-wavelength detection, or using multiple microfluidic channels contacting a single Snapwell insert (see Supplementary Video 3). Also, it is possible to do time-lapse imaging on single cell cultures, including consecutive measurements for different physiological conditions by programmed injection of different perfusates, in which epithelia

Author Manuscript Author Manuscript Author Manuscript Author Manuscript

integrity can be maintained for many hours using sterile solutions and an environment chamber. Finally, transepithelial fluid transport and permeability measurements should be possible in living intact tissues ex vivo or in vivo.

Though many applications of the FT-on-Chip method are possible, several limitations are noted. Measurements require an intact epithelial cell layer cultured on a porous membrane without defects. The fluorophore selected as a volume indicator or sensor should not undergo self-quenching or photobleaching, or produce phototoxicity. Because the fluorescence profile is determined from the properties of all cells overlying the microfluidic channel, heterogeneity in cell-to-cell properties is averaged. The time resolution of FT-on-Chip method is related to the time required to generate a steady-state axial fluorescence profile, which may take up to several minutes depending on perfusion rate. Another general limitation, which applies to any type of transepithelial transport measurement across filter-grown epithelial cell layers, is the possibility of unstirred layer effects, which might occur for high permeability rates and when filter pore size is small and pore density is low. Another general limitation is the possibility of paracellular leakage of solutes if an epithelium is or becomes leaky in response to an osmotic or solute gradient, which if not taken into account would produce inaccurate permeability values. Finally, parallel measurements in separate wells are not easily implemented.

## Conclusion

FT-on-Chip provides a simple solution to the problem of measuring transepithelial permeability and fluid transport with high time resolution using standard laboratory cell culture filters and a low-magnification fluorescence imaging system. The method is generalizable to many types of water and solute transport measurements for which a fluorescent indicator method can be applied, and multiplexed studies are possible measuring several parameters simultaneously. The method should also be applicable to transepithelial permeability measurements in tissues in vivo, such as exposed urinary bladder or intestine, in which the apical surface contacts the microfluidic channel and basolateral perfusion is unnecessary because of blood flow.

## Supplementary Material

Refer to Web version on PubMed Central for supplementary material.

## Acknowledgments

This work was supported by grants DK72517, DK099803, EB00415, DK101373, DK35124, and EY13574 from the National Institutes of Health, and grants from the Cystic Fibrosis Foundation and Guthy-Jackson Charitable Foundation.

## References

1. Carbrey JM, Agre P. Exp Pharmacol. 2009; 190:3–28.
2. Verkman AS. Annu Rev Med. 2012; 63:303–16. [PubMed: 22248325]
3. Verkman AS, Anderson MO, Papadopoulos MC. Nat Rev Drug Disc. 2014; 13:259–77.
4. Frigeri A, Nicchia GP, Svelto M. Curr Pharm Des. 2007; 13:2421–7. [PubMed: 17692010]

Author Manuscript Author Manuscript Author Manuscript Author Manuscript

5. Jeyaseelan K, Sepramaniam S, Armugam A, Wintour EM. Expert Opin Ther Targets. 2006; 10:889–909. [PubMed: 17105375]
6. Solenov E, Watanabe H, Manley GT, Verkman AS. Am J Physiol. 2004; 286:C426–32.
7. Baumgart F, Rossi A, Verkman AS. J Gen Physiol. 2012; 139:83–91. [PubMed: 22200949]
8. Jin BJ, Esteva-Font C, Verkman AS. Lab Chip. 2015; 15:3380–90. [PubMed: 26159099]
9. Levin MH, Sullivan S, Nielson D, Yang B, Finkbeiner WE, Verkman AS. J Biol Chem. 2006; 281:25803–12. [PubMed: 16829520]
10. Yang B, Kim KK, Verkman AS. FEBS Lett. 2006; 580:6679–84. [PubMed: 17126329]
11. Law CS, Candia OA, To CH. Invest Ophthalmol Vis Sci. 2009; 50:1299–306. [PubMed: 18824735]
12. Matsui H, Davis CW, Tarran R, Boucher RC. J Clin Invest. 2000; 105:1419–27. [PubMed: 10811849]
13. Song Y, Namkung W, Nielson DW, Lee JW, Finkbeiner WE, Verkman AS. Am J Physiol Lung Cell Mol Physiol. 2009; 297:L1131–40. [PubMed: 19820035]
14. Hays RM, Leaf A. J Gen Physiol. 1962; 45:905–19. [PubMed: 13905689]
15. Li L, Zhang H, Verkman AS. Am J Physiol. 2009; 296:G816–22.
16. Miller SS, Hughes BA, Machen TE. Proc Natl Acad Sci U S A. 1982; 79:2111–5. [PubMed: 6177005]
17. Brahm J. J Gen Physiol. 1982; 79:791–819. [PubMed: 7097244]
18. Burg MB. Kid Internatl. 1982; 22:417–24.
19. Schafer JA, Andreoli TE. J Clin Invest. 1972; 51:1264–78. [PubMed: 5057131]
20. Kuwahara M, Berry CA, Verkman AS. Biophys J. 1988; 54:595–602. [PubMed: 3224145]
21. Xia Y, Whitesides GM. Annu Rev Mater Sci. 1998; 28:153–184.
22. McDonald JC, Duffy DC, Anderson JR, Chiu DT, Wu H, Schueller OJA, Whitesides GM. Electrophoresis. 2000; 21:27–40. [PubMed: 10634468]
23. Kuwahara M, Verkman AS. Biophys J. 1988; 54:587–93. [PubMed: 3224144]
24. Saadoun S, Papadopoulos MC, Hara-Chikuma M, Verkman AS. Nature. 2005; 434:786–92. [PubMed: 15815633]
25. Tradtrantip L, Tajima M, Li L, Verkman AS. J Med Invest. 2009; 56:179–84. [PubMed: 20224178]
26. Preisig P, Berry C. Am J Physiol Renal Physiol. 1985; 249:F124–F141.
27. Lo CM, Keese CR, Giaever I. Exper Cell Res. 1999; 250:576–80. [PubMed: 10413610]

Author Manuscript Author Manuscript Author Manuscript Author Manuscript

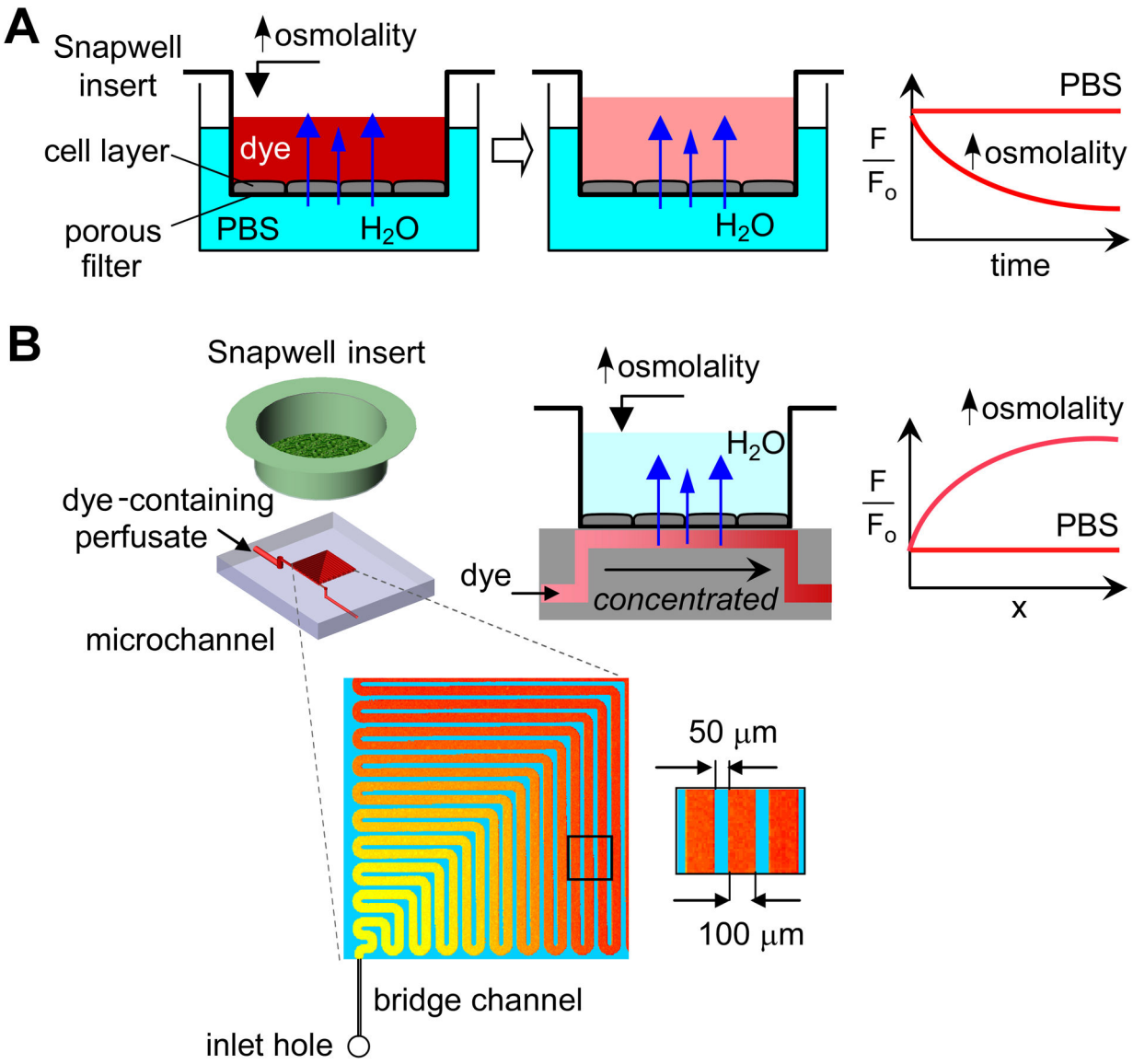


**Figure 1.**

Conventional and FT-on-Chip measurement of transepithelial osmotic water permeability of cells grown on a Snapwell insert with porous filter. **A**. Conventional dye dilution method in which osmotic water transport is deduced using a volume marker in the apical bathing solution. A transepithelial osmotic gradient is established using solutions of different osmolalities on opposite sides of the cell layer. Dye concentration is measured in serial fluid samples. **B**. FT-on-Chip method in which a long, shallow microchannel in contact with the porous membrane of a Snapwell insert containing the cell layer is perfused with a membrane-impermeable fluorescent dye. Water transport results in dilution or concentration of the fluorescent dye along the length of the channel, as measured from a single full-field fluorescence image. (top left and center) Schematic showing Snapwell insert and microchannel, (top right) predicted relative fluorescence along the axis (x-direction) of the channel, and (bottom) diagram of microfluidic channel of dimensions 3.2 × 3.2 $mm^2$, with

channel width 100 μm, height 20 μm, and length 10 cm. The bridge channel dimensions are width 25 mm and length < 1 mm.

Author Manuscript Author Manuscript Author Manuscript Author Manuscript

Author Manuscript Author Manuscript Author Manuscript Author Manuscript

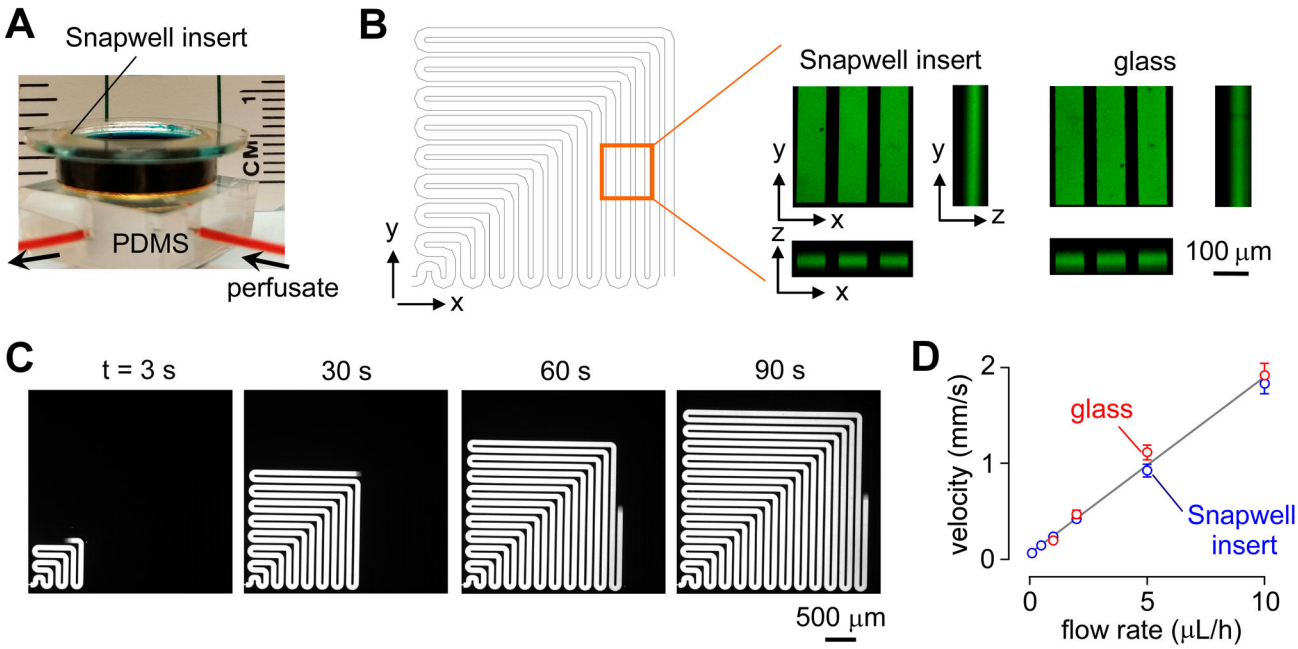


**Figure 2.**

Characterization of microfluidic channel. **A**. Photograph of FT-on-Chip device (without the 50-g weight on top for better viewing) showing Snapwell insert overlying the microfluidic channel, which rests on a glass slide. **B**. Confocal fluorescence images of the microfluidic channel (containing PBS with fluorescein dextran) measured using a 10× lens, in contact with a Snapwell insert (containing cultured cells) or a glass coverslip. **C**. Filling of the microchannel during perfusion with PBS containing fluorescein dextran at 10-μL/h flow rate (also see Supplementary Video S1). **D**. Velocity of 1-μm diameter fluorescent beads in the perfusate as a function of perfusion rate as measured by Particle Streak Velocimetry (mean ± S.E.M., n=50). Measurements made with Snapwell insert containing cells or a glass coverslip.

Author Manuscript Author Manuscript Author Manuscript Author Manuscript

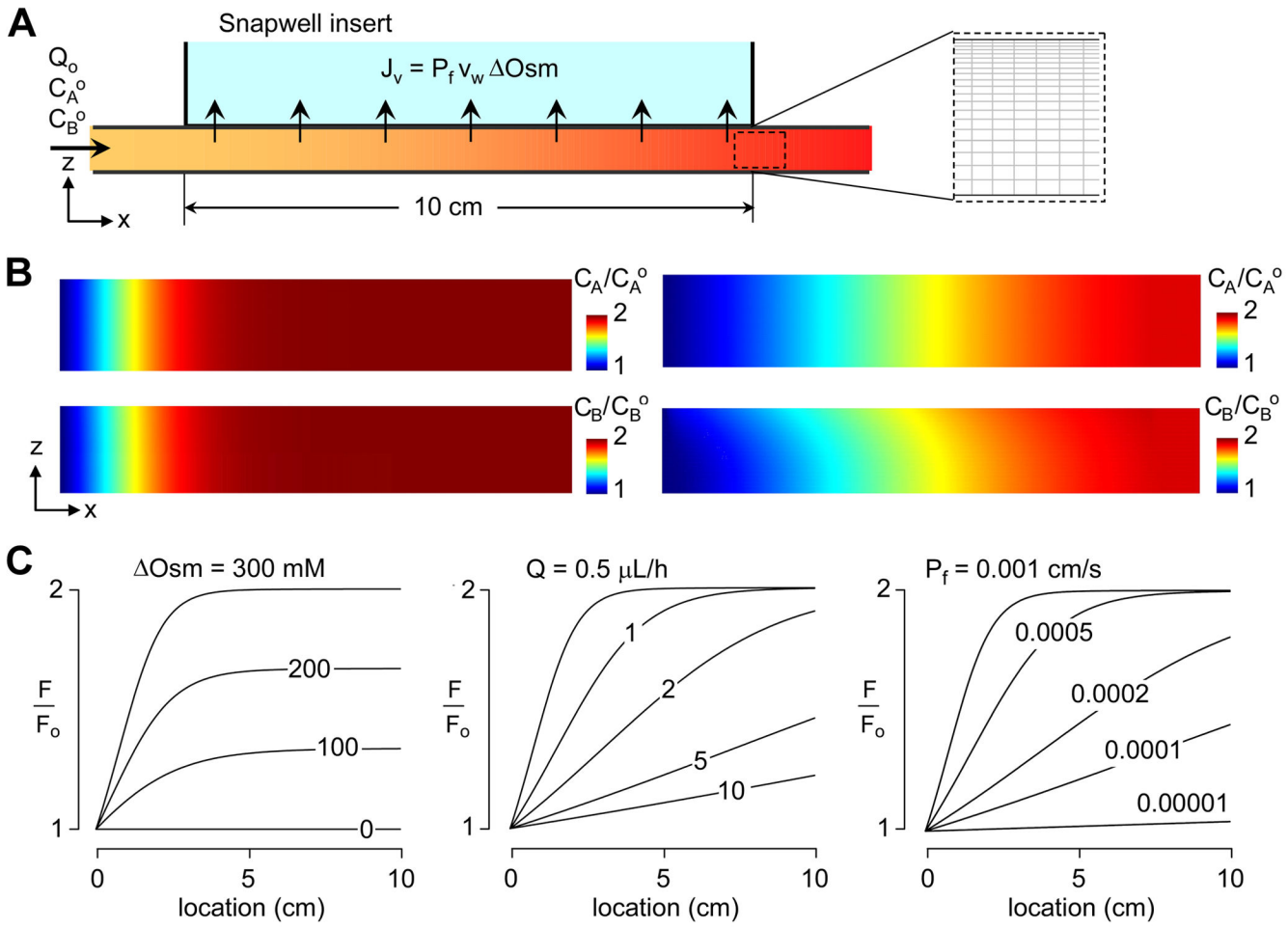


**Figure 3.**

Computational determination of fluorescence profiles in the microchannel in response to a transepithelial osmotic gradient. **A**. Schematic with inlet boundary conditions ($C_A$ = 300 mM, $C_B$ = 10 μM, Q = 0.5 μl/h), advective outlet boundary conditions ($\nabla C_A = \nabla C_B = 0$), and volume flux boundary condition through a 10-cm-long channel bounded by a porous membrane (see Supplementary Information for computational details). A 1-mm length entrance was used to generate a fully developed velocity field for computations. **B**. Pseudocolor profiles of solute A and dye B in the microchannel for $P_f$ = 0.001 cm/s, perfusate flow = 0.5 μL/h, ΔOsm = 300 mM, and diffusion coefficients $D_A = 10^{-9}$ $m^2/s$ and $D_B = 5\times10^{-10}$ $m^2/s$ (left); and for $P_f$ = 0.001 cm/s, perfusate flow = 2 μL/h, ΔOsm = 300 mM, $D_A = 10^{-9}$ $m^2/s$, and $D_B = 5\times10^{-11}$ $m^2/s$ (right). **C**. (left) Relative fluorescence along the microchannel for the indicated osmotic gradients with $P_f$ = 0.001 cm/s and perfusate flow = 0.5 μL/h (left); for the indicated injection flow rates with $P_f$ = 0.001 cm/s and ΔOsm = 300 mM (center); and for indicated osmotic water permeability ($P_f$) with ΔOsm = 300 mM and perfusate flow = 0.5 μL/h (right).

Author Manuscript Author Manuscript Author Manuscript Author Manuscript

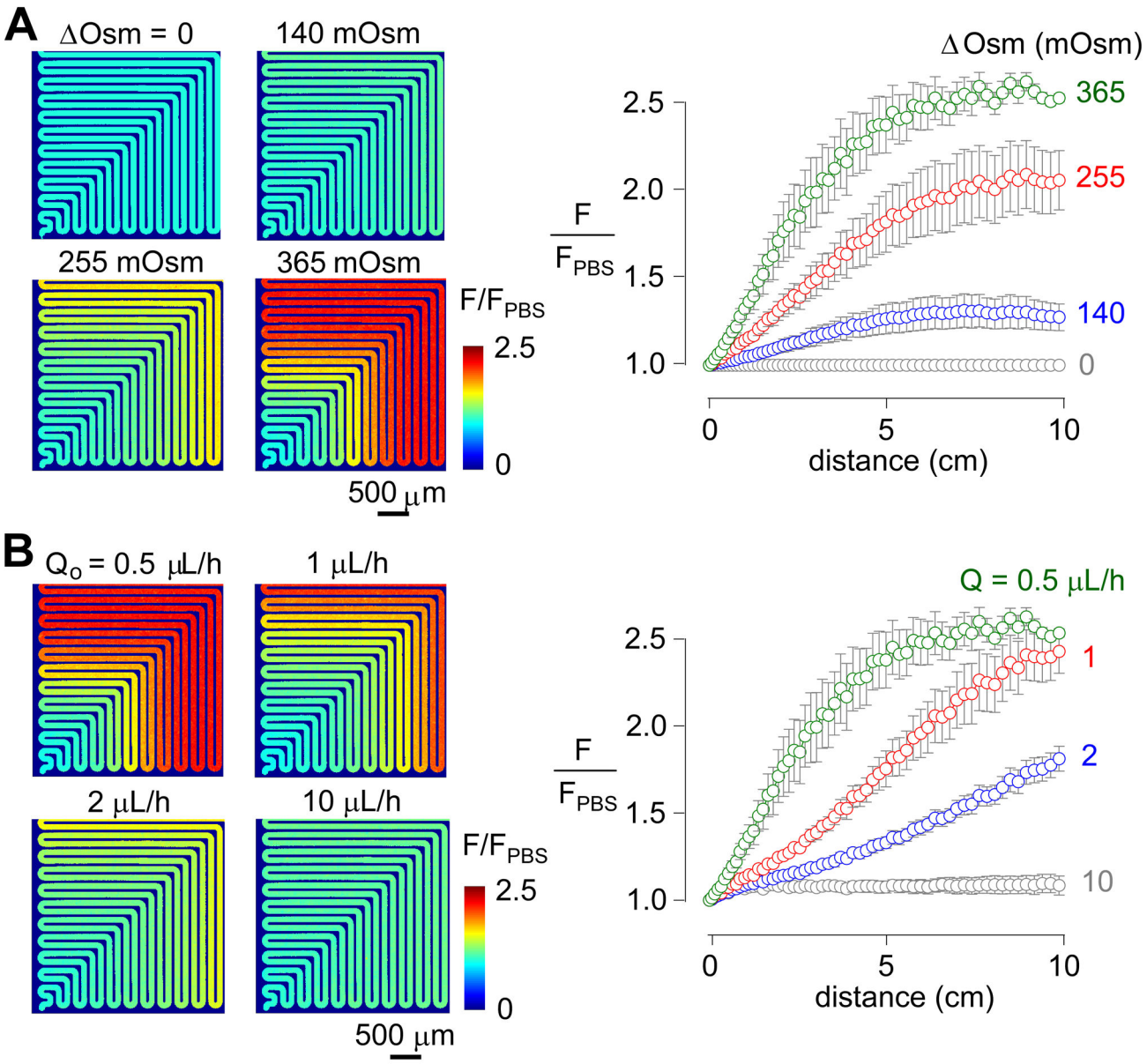


**Figure 4.**

Spatial fluorescence profiles in the microchannel in response to a transepithelial osmotic gradient. **A**. (left) Pseudocolor images of channel fluorescence in the absence of an osmotic gradient (PBS in solution overlying cells) and with different osmotic gradients produced by addition of raffinose in the solution overlying the cell layer. Perfusion flow rate was 0.5 μl/h. (right) Spatial fluorescence profiles from images in Fig. 4A. Each point is mean ± S.E.M., n=3. **B**. (left) Pseudocolor images of channel fluorescence in response to a 365-mM osmotic gradient for different perfusion flow rates. (right) Spatial fluorescence profiles from images in Fig. 4B.

Author Manuscript Author Manuscript Author Manuscript Author Manuscript

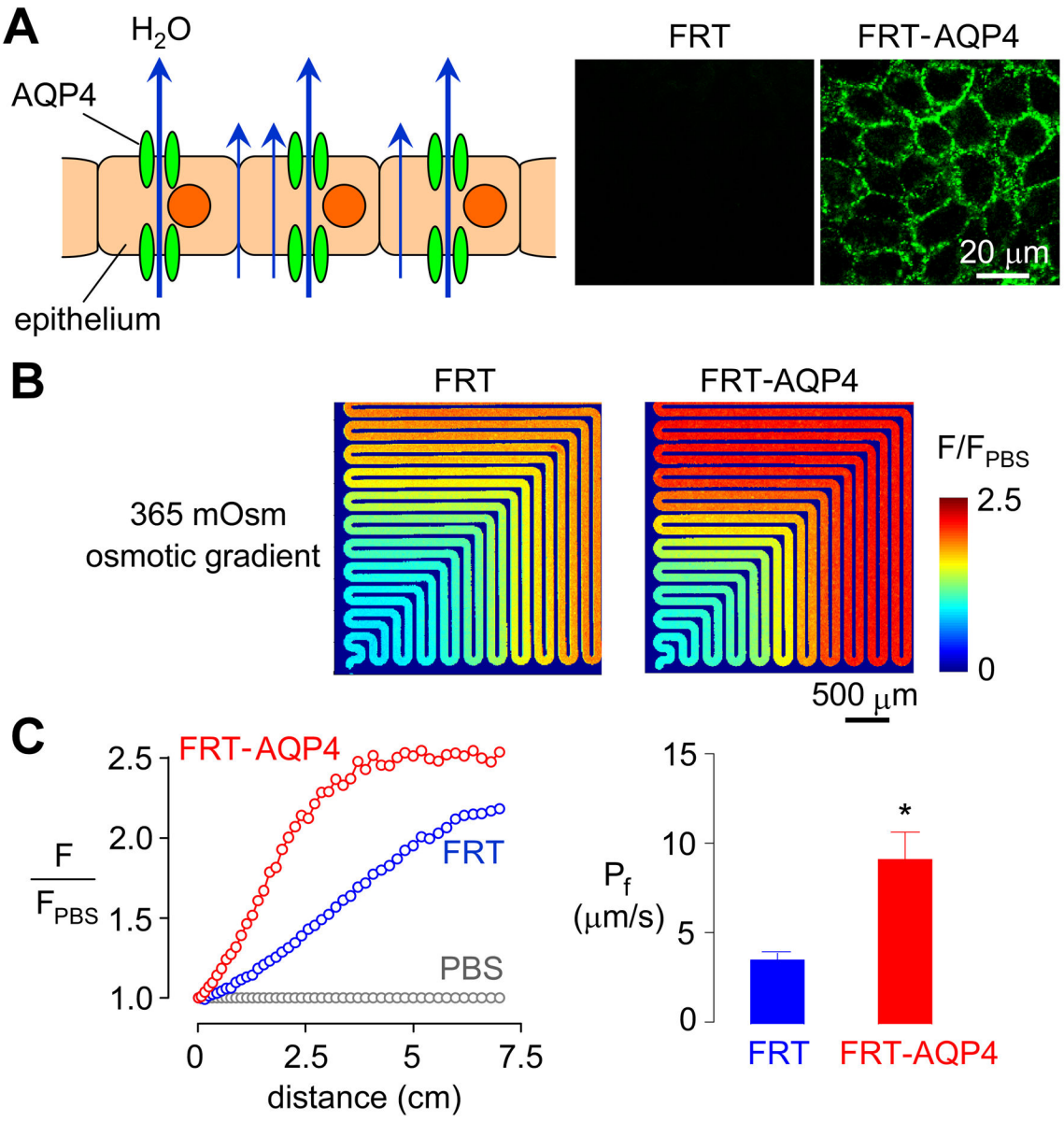


**Figure 5.**

Transepithelial osmotic water permeability in FRT cells expressing AQP4 water channels. A. (left) Schematic of AQP4-facilitated transepithelial water transport, showing water movement through AQP4 as well as non-AQP4 transcellular and paracellular routes. (right) AQP4 immunofluorescence (green) in (non-transfected) FRT and FRT-AQP4 cells. B. Pseudocolor images of microchannel fluorescence for a 365-mM osmotic gradient in (non-transfected) FRT and FRT-AQP4 cells for perfusate flow of 0.5 μL/h. C. (left) Deduced spatial fluorescence profiles from images in Fig. 5B. (right) Transepithelial osmotic water permeability ($P_f$) (mean ± S.E.M., n=6, * $P < 0.001$).

Author Manuscript Author Manuscript Author Manuscript Author Manuscript

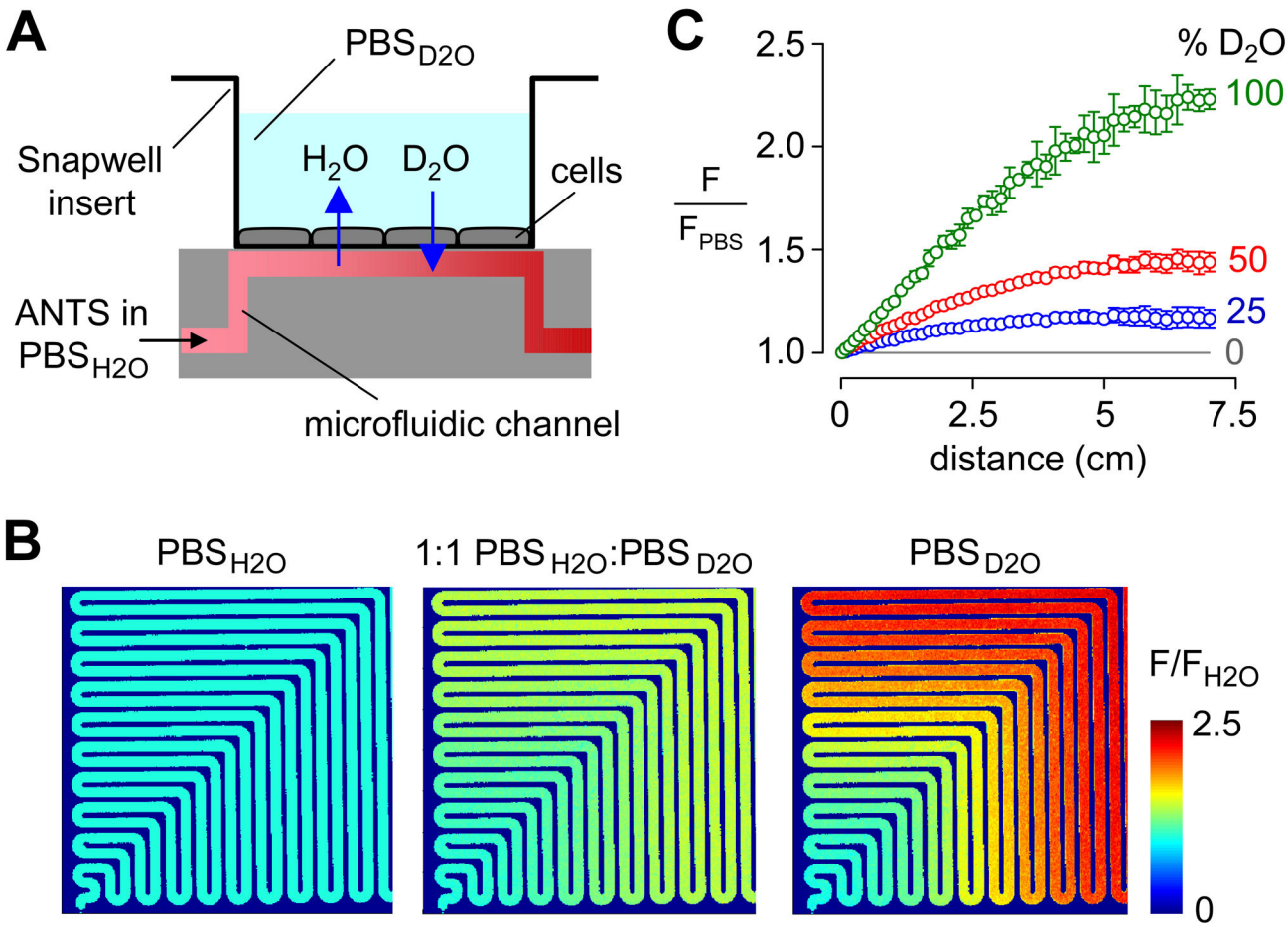


**Figure 6.**

Transepithelial diffusional permeability in FRT cells. **A**. Schematic showing diffusional movement of $D_2O$ across an epithelial monolayer (in exchange for $H_2O$) in the absence of an osmotic gradient. A $D_2O$-sensitive membrane-impermeant fluorophore (aminonapthalene trisulfonic acid, ANTS) in PBS is perfused through the microchannel. **B**. Pseudocolor images of microchannel fluorescence for isosmolar solutions of different $D_2O$ percentages overlying the epithelial layer for perfusate flow rate of 5 μL/h. **C**. Deduced spatial fluorescence profiles from images in Fig. 6B.